Published in final edited form as:
Mol Cell. 2010 March 26; 37(6): 797–808. doi:10.1016/j.molcel.2010.02.022.

Postnatal deamidation of 4E-BP2 in brain enhances its association with raptor and alters kinetics of excitatory synaptic transmission

Michael Bidinosti[1], **Israeli Ran**[2,*], **Maria R. Sanchez-Carbente**[3,*], **Yvan Martineau**[1,*], **Anne-Claude Gingras**[4], **Christos Gkogkas**[1], **Brian Raught**[5], **Clive Bramham**[6], **Wayne S. Sossin**[7], **Mauro Costa-Mattioli**[1,8], **Luc DesGroseillers**[3], **Jean-Claude Lacaille**[2], and **Nahum Sonenberg**[1]

[1]Department of Biochemistry and Goodman Cancer Centre, McGill University, Montréal, QC H3G 1Y6, Canada

[2]Département de Physiologie, Université de Montréal, Montréal, QC H3C 3J7, Canada

[3]Département de Biochimie, Université de Montréal, Montréal, QC H3C 3J7, Canada

[4]Samuel Lunenfeld Research Institute and Department of Molecular Genetics, University of Toronto, Toronto, ON M5G 1X5, Canada

[5]Ontario Cancer Institute, McLaughlin Centre for Molecular Medicine and Department of Medical Biophysics, University of Toronto, Toronto, ON M5G 1L7, Canada

[6]Department of Biomedicine and Bergen Mental Health Research Center, University of Bergen, 5009 Bergen, Norway

[7]Department of Neurology and Neurosurgery, Montreal Neurological Institute, McGill University, Montréal, QC H3A 2B4, Canada

Summary

The eIF4E-binding proteins (4E-BPs) repress translation initiation by preventing eIF4F complex formation. Of the three mammalian 4E-BPs, only 4E-BP2 is enriched in the mammalian brain and plays an important role in synaptic plasticity and learning and memory formation. Here we describe asparagine deamidation as brain-specific posttranslational modification of 4E-BP2. Deamidation is the spontaneous conversion of asparagines to aspartates. Two deamidation sites were mapped to an asparagine-rich sequence unique to 4E-BP2. Deamidated 4E-BP2 exhibits increased binding to the mammalian Target of Rapamycin (mTOR)-binding protein raptor, which effects its reduced association with eIF4E. 4E-BP2 deamidation occurs during postnatal development, concomitant with the attenuation of the activity of the PI3K-Akt-mTOR signalling pathway. Expression of deamidated 4E-BP2 in 4E-BP2−/− neurons yielded mEPSCs exhibiting increased charge transfer with slower rise and decay kinetics, relative to the wild type form. 4E-BP2 deamidation may represent a compensatory mechanism for the developmental reduction of PI3K-Akt-mTOR signalling.

Correspondence: nahum.sonenberg@mcgill.ca.
[8]Present Address: Department of Neuroscience, Baylor College of Medicine, Houston, TX 77030, USA
[*]These authors contributed equally to this work.

Introduction

Eukaryotic protein synthesis is primarily controlled at the initiation phase. A critical early event in this process is the association of the eukaryotic initiation factor 4E (eIF4E) with the mRNA 5′ m^7GpppN-cap structure. eIF4E associates with eIF4G and eIF4A, to form the three-subunit eIF4F complex, which facilitates 40S ribosome recruitment to the mRNA 5′ end (Gingras et al., 1999b; Pestova et al., 2007). In mammals, an important regulatory function in this process is carried out by the eIF4E-binding proteins. The members of this family of three paralogs (4E-BP1, 2, and 3) compete with eIF4G for the same binding site on the dorsal surface of eIF4E (Mader et al., 1995; Marcotrigiano et al., 1999), and thereby inhibit translation initiation by preventing the interaction of eIF4E with eIF4G (Haghighat et al., 1995). The association of the 4E-BPs with eIF4E is abrogated by their hierarchical, multi-site phosphorylation (Gingras et al., 2001a; Mothe-Satney et al., 2000). The 4E-BPs exhibit disparate tissue expression (Lin and Lawrence 1996; Tsukiyama-Kohara et al. 2001). 4E-BP2 is predominant in the brain and its requirement for learning and memory has been studied extensively. Deletion of 4E-BP2 in mice engenders hippocampus-dependent memory impairments and alterations in long-lasting forms of synaptic plasticity (Banko et al., 2006; Banko et al., 2007; Banko et al., 2005).

The eIF4E-binding activity of the 4E-BPs is regulated through phosphorylation by the mammalian target of rapamycin complex 1 (mTORC1) (Gingras et al., 2001b; Proud, 2009; Yonezawa et al., 2004). In addition to the large serine/threonine kinase mTOR, this complex consists of GβL (LST8), and the mTORC1-defining member, raptor. Raptor, is a large scaffolding protein that recruits mTORC1 substrates to the mTOR kinase domain through interaction with a substrate-specific TOR signaling (TOS) motif (Ma and Blenis, 2009). In 4E-BPs, the C-terminal TOS motif is necessary for binding to raptor and, consequently, for phosphorylation leading to their release from eIF4E (Nojima et al., 2003; Schalm et al., 2003). However, recent studies have indicated that the TOS motif alone is insufficient for efficacious 4E-BP1-raptor binding, thereby suggesting that other sequences in the 4E-BPs enhance this interaction (Choi et al., 2003; Eguchi et al., 2006; Lee et al., 2008).

mTOR stimulates cell growth and proliferation (Sarbassov et al., 2005). mTOR integrates inputs from several signaling cascades communicating extracellular stimuli (PI3K-Akt pathway), intracellular energy status (LKB1-AMPK), cellular stresses (virus infection and hypoxia), and nutrient availability (Rag GTPases) into growth-promoting outputs, in particular protein synthesis (Sancak and Sabatini, 2009; Wullschleger et al., 2006). In neuronal systems, mTOR modulates several processes, including learning and memory (Ehninger et al., 2008; Parsons et al., 2006), synaptic plasticity (Cammalleri et al., 2003; Tang et al., 2002), dendritic protein synthesis (Gobert et al., 2008; Takei et al., 2004; Tsokas et al., 2005), and formation of the dendrite arbor (Jaworski et al., 2005; Kumar et al., 2005). However, recent work demonstrated that mTORC1 activity declines during postnatal development in retinal ganglion neurons (Park et al., 2008).

Here we describe a brain-specific posttranslational modification of 4E-BP2. In the mammalian brain two C-terminal asparagines were found to undergo developmentally regulated deamidation to aspartates. This resulted in enhanced association with raptor and reduced translational repression. Expression of the deamidated form of 4E-BP2 in neurons altered the time course of excitatory synaptic activity. We suggest that 4E-BP2 deamidation may act as a compensatory mechanism to promote translation despite attenuated PI3K-Akt- mTOR signalling in neuron development.

Results

4E-BP2 in Mammalian Brain Resolves into Three Forms Independent of Phosphorylation

4E-BP2 from murine brain migrates in SDS-PAGE as three forms (Banko et al., 2005; Tsukiyama-Kohara et al., 2001) that are reminiscent of the multi-site phosphorylated species of 4E-BP1 (Gingras et al., 1999a; Lin et al., 1994). Considering the role of 4E-BP2 in synaptic plasticity and learning and memory processes (Banko et al., 2006; Banko et al., 2007; Banko et al., 2005), we wished to study its regulation by phosphorylation in the mammalian nervous system. We first determined whether the hierarchical mode of 4E-BP1 phosphorylation, in which Thr37 and Thr46 phosphorylation precedes Thr70 and Ser65, is maintained in 4E-BP2. This was confirmed as 4E-BP2 Thr37Ala or Thr46Ala variants exhibited impaired hyperphosphorylation, relative to Thr70Ala or wild type proteins (Figure S1). Surprisingly, we were unable to detect significant levels of phosphorylated 4E-BP2 in adult whole brain or hippocampal extracts by Western blotting (Figures 1A and S1). Moreover, the slowest-migrating form is specific to the brain. If the migration pattern of brain-derived 4E-BP2 is due to hyperphosphorylation one might expect reduced or abolished association with eIF4E, as is the case for hyperphosphorylated 4E-BP1. However, Far Western (FW) blotting with radiolabeled eIF4E on the brain lysates of wild type and 4E-BP2 null mice revealed that eIF4E bound similarly to each of the three 4E-BP2 species (Figure 1B). Further, phosphatase treatment of brain extract failed to alter the pattern of 4E-BP2 migration (Figure 1C). Thus, these slow-migrating forms are not due to hyperphosphorylation

Asparagine Deamidation Causes the Slow Migrating Forms of 4E-BP2 in the Brain

No alternatively spliced 4E-BP2 transcripts have been identified; therefore, the possibility that an uncharacterized posttranslational modification accounts for the slow-migrating 4E-BP2 forms in the brain was probable. To identify this modification, endogenous 4E-BP2 was purified from adult murine brains and mass spectrometry was performed. This analysis detected deamidation, the non-enzymatic conversion of asparagine to aspartate, near the C-terminus (Figure S2). The deamidation process is largely influenced by the identity of the adjacent C-terminal residue (Robinson et al., 1973; Robinson and Robinson, 2001) and the proximity to flexible peptide regions (Xie and Schowen, 1999). The rate of deamidation is also increased under alkaline conditions, thus facilitating analysis of susceptible residues (Robinson and Rudd, 1974). Purified recombinant 4E-BP2 was therefore treated over a range of alkalinity. Incubation for six hours elicited a single, slower migrating form, while an additional species was noticed upon protracted incubation at higher pH (Figure 2A). Bcl-X_L also exhibits reduced electrophoretic mobility upon aspargine deamidation (Deverman et al. 2002). To confirm that deamidation is the 4E-BP2 modification found in the brain, mouse embryonic fibroblasts (MEFs) were starved of serum and amino acids to minimize phosphorylation, and cell lysates were then subjected to alkaline conditions. A 4E-BP2 migration pattern, similar to that described above (Figure 2A), was observed following alkaline treatment (Figure 2B), and was identical to that of brain lysates in both SDS-PAGE (Figure S2) and IEF/SDS-PAGE (Figure 2C; second and third panels). Strikingly, the 4E-BP2 IEF/SDS-PAGE spots were perfectly superimposed when the MEF and brain lysates were mixed, thereby confirming uniform modification (Figure 2C; fourth panel). Thus, 4E-BP2 in the brain is modified by asparagine deamidation.

Asparagines 99 and 102 are the Sites of 4E-BP2 Deamidation

We questioned whether asparagine deamidation is unique, amongst the 4E-BPs, to 4E-BP2. 4E-BP2 contains six closely-spaced asparagines near its C-terminus that are not conserved in 4E-BP1 (Figure 3A). Incubation of MEF lysates at alkaline pH caused a partial reduction in 4E-BP2 migration that was not observed for 4E-BP1 (Figure 3B). As deamidation appears to be unique to 4E-BP2, we next sought to identify the modified sites. First, 3HA-tagged wild

type 4E-BP2 and a variant lacking the asparagine-rich sequence (Δ87-104) were expressed in HEK293 cells and subjected to alkaline treatment. The deletion variant exhibited no reduction in electrophoretic mobility following incubation at pH 10, confirming that 4E-BP2 deamidation occurs at this region (Figure 3C; note that the 3HA-tagged proteins do not migrate in a pattern similar to endogenous 4E-BP2).

IEF/SDS-PAGE analysis of 4E-BP2 revealed two deamidated forms in the adult brain (Figure 2C). We therefore determined the major deamidation sites within the asparagine-rich stretch. To do so, recombinant 4E-BP2 was treated at high pH and the resolved species (Figure 3D; left panel) were analyzed by mass spectrometry. Because deamidation is non-enzymatic and an intrinsic property of an asparagine within a peptide, the susceptible residues determined in this analysis correspond to those occurring *in vivo*. A clear preference for aspartate formation was observed at positions 99 and 102 (Figures 3D and S3). Mutating both of these residues to alanines (N99A/N102A) confirmed this finding as it prevented the alkaline-induced deamidation shift (Figure 3E). Asparagines 99 and 102 were then mutated to aspartates to replicate *in vivo* deamidation. Electrophoretic mobility was reduced to a similar extent by the N99D and N102D variants and even more so by N99D/N102D (Figure 3F), the form unique to the brain.

Deamidated 4E-BP2 Exhibits Enhanced Raptor-Binding and Reduced eIF4E-Association

We considered the possibility that the proximity of the deamidation sites to the C-terminal TOR signaling (TOS) motif might affect the interaction of 4E-BP2 with raptor. This is plausible in light of recent findings that the TOS motif in 4E-BP1 alone can not account for efficient raptor-binding (Lee et al., 2008). After co-transfection, more deamidated (N99D/N102D) 4E-BP2 co-immunoprecipitated with raptor in comparison to wild type or 4E-BP2 N99A/N102A (Figure 4A). Deletion of the TOS motif from 4E-BP2 (ΔTOS) abolished its interaction with raptor. We then wondered whether 4E-BP2 deamidation affects its *in vivo* interaction with eIF4E. Deamidated 4E-BP2 exhibited reduced association with eIF4E recovered on an mRNA cap-analogue (m^7GDP) resin (Figure 4B). As 4E-BP2 phosphorylation was not detected in mature brain, the association of 4E-BP2 and eIF4E was monitored in conditions favouring diminished 4E-BP2 phosphorylation owing to reduced mTORC1-activation. In the absence of serum (-FBS) alone or of serum and nutrients (PBS) together, a marked reduction in eIF4E-bound deamidated 4E-BP2 was still observed (Figures 4C and 4D). This effect was dependent on interaction with raptor as deamidated 4E-BP2 lacking the TOS motif (N99D/N102D/ΔTOS) displayed a greater or equal association with eIF4E relative to wild type 4E-BP2 (Figure 4D). These findings were confirmed *in vivo* in the brain; comparison of the ratio of deamidated 4E-BP2 to unmodified 4E-BP2 between m^7GDP pulldowns and brain lysates indicated that more unmodified 4E-BP2 (fastest migrating form) was recovered with eIF4E than were the deamidated forms (Figure 4E). In agreement with these findings, prior work showed that mutation of the TOS motif enhanced 4E-BP1 association with eIF4E (Schalm et al., 2003; Wang et al., 2006). We also confirmed that the association of deamidated 4E-BP2 with raptor increased under conditions of reduced mTORC1 activity (Figure S4). Far Western analysis on brain lysates (Figure 1C) or recombinant proteins (Figure 4F) yielded similar eIF4E-binding to wild type or deamidated 4E-BP2. However, as these assays involve the direct interaction between eIF4E and non-phosphorylated 4E-BP2 in the absence of raptor, the results are consistent with the above finding that the weakened association of deamidated 4E-BP2 with eIF4E is effected by raptor.

We then tested the capacity of deamidated 4E-BP2 to repress translation. To do so, we first used a luciferase reporter mRNA harbouring a 4E-BP-sensitive 5′ untranslated region (5′UTR), which contains extensive secondary structure (ΔG = −137kCal/mol), obtained from the mRNA of IRF-7 (Interferon Regulatory Factor 7) (Colina et al., 2008). In MEFs lacking 4E-BP1 and

4E-BP2, expression of deamidated 4E-BP2 repressed translation of the reporter mRNA weakly in comparison to wild type 4E-BP2 (Figure 4G). Importantly, the control luciferase mRNA that contains weak secondary structure was not significantly inhibited by either deamidated or wild type 4E-BP2 (Figure S4). We similarly observed in 4E-BP2−/− cultured neurons that deamidated 4E-BP2 weakly repressed, relative to wild type 4E-BP2, the translation of a previously characterized fluorescence-based reporter mRNA (Figure 4H). This mRNA contains significant secondary structure in the 5′UTR (ΔG = −55kCal/mol), which is derived from CaMKIIα mRNA. Translational expression from this reporter has been shown to be induced by activity and is normally weak in dendrites distal to the cell body in unstimulated conditions (Aakalu et al., 2001; Gong et al., 2006). Thus, our basal level measurements were restricted to a proximal dendrite region (15-30μm from the cell body). Anisomycin treatment confirmed that translation represents a significant component of expression from this reporter mRNA in our assay. Overall, these experiments suggest that deamidated 4E-BP2 is a weak repressor of translation by virtue of its enhanced association with raptor.

Developmental Reduction in PI3K-Akt-mTOR Signaling is Associated with the Onset of 4E-BP2 Deamidation

The absence of phosphorylated 4E-BP2 in the mature brain is at variance with reports of robust 4E-BP phosphorylation in *ex vivo* dissociated neuron cultures (Kelleher et al., 2004; Takei et al., 2001). These cultures are normally prepared from embryonic or early postnatal brains; therefore, a developmental regulation of 4E-BP2 phosphorylation was considered. 4E-BP2 phosphorylation sharply receded during the first two weeks of postnatal brain development [postnatal days (P) 3, 7 and 15; Figure 5A]. Concomitantly, the slow migrating deamidated forms of 4E-BP2 became apparent with time. IEF/SDS-PAGE analysis of the P3 lysate confirmed the stoichiometric abundance of phosphorylated 4E-BP2 species (horizontal pattern) (Figure 5B). However, between one and three postnatal weeks, 4E-BP2 phosphorylation decreased, while the appearance of the deamidated forms (diagonal pattern) became apparent (Figure 5C). Phosphatase treatment of the P15 lysate abolished the horizontal pattern (Figure 5D), thereby confirming its assignment as multiple phosphorylation events. Alkaline treatment of the P3 lysate induced the appearance of the doubly deamidated (N99D/N102D) form that is normally present in the adult (Figure S5).

We next asked whether the PI3K-Akt-mTOR signaling module was affected during development. Brain lysates from P3 and adult mice were examined along with lysates from dissociated hippocampal neuron cultures at several days following plating (days *in vitro*; DIV). The phosphorylation of both Akt and ribosomal protein S6 (rpS6), a downstream target of mTORC1, were dramatically reduced in the adult brain relative to P3. This effect was mirrored in cultured neurons between days 9 and 31 (Figure 5E). Diminished rpS6 phosphorylation was also observed recently during development of retinal ganglion neurons (Park et al., 2008). Importantly, 4E-BP2 deamidation was also observed in the cultured preparations (Figure 5E; top panel). These observations, together with the raptor-dependent reduction of eIF4E-binding (Figures 4C and 4D) and weak translation repression (Figures 4G and 4H), suggest the possibility of a compensatory function for 4E-BP2 deamidation to permit protein synthesis despite reduced, translation-promoting upstream signaling. In support of this putative function, we found that the eIF4F complex, which is formed between eIF4E and eIF4G during translation initiation and is antagonized by 4E-BPs, remained effectively associated during the developmental period in which 4E-BP2 deamidation occurs (Figure 5F). Accordingly, deamidated 4E-BP2 was weakly associated with eIF4E (Figure 5F).

Expression of Deamidated 4E-BP2 in 4E-BP2−/− Neurons Alters the Kinetics of Excitatory Synaptic Transmission

4E-BP2 knock-out mice display altered hippocampal long-term synaptic plasticity (Banko et al. 2005, 2006). We therefore wondered whether 4E-BP2 deamidation impacts excitatory postsynaptic transmission. To pursue this, AMPA receptor-mediated miniature excitatory postsynaptic currents (mEPSCs) were recorded at the soma of CA1 pyramidal neurons in organotypic slice cultures. These phenomena represent the postsynaptic current produced by the presynaptic release of single glutamate vesicles. As a rule, mEPSC amplitude largely reflects the number of AMPA receptors in the postsynaptic membrane, frequency depends on both the probability of presynaptic transmitter release and the number of active synapses, while charge transfer is the cumulative ion flow through open receptor channels (Lisman et al., 2007). First, mEPSCs were compared between wild type and 4E-BP2−/− slices. 4E-BP2−/− neurons exhibited approximately a two-fold increase in mEPSC amplitude, frequency, and charge transfer relative to wild type controls (Figure 6A). The increases in amplitude and charge transfer were not due to differences in cell cable properties or recording quality, because series and input resistance and cell capacitance were not different between wild type and 4E-BP2−/− neurons (Figure S6). Thus, excitatory synaptic activity is increased in the absence of 4E-BP2. Next, wild type or deamidated 4E-BP2 (N99D/N102D) proteins were expressed in 4E-BP2−/− neurons to examine their specific functions. mEPSC amplitude and frequency were similarly repressed by expression of either protein (Figure 6B). However, mEPSC charge transfer was only partially rescued by 4E-BP2 N99D/N102D. This incomplete repression suggests that deamidated 4E-BP2 has an altered effect on mEPSC kinetics. Indeed, upon expression of deamidated 4E-BP2, mEPSPs exhibited strikingly slower rise and decay times in comparison to control (Figure 6C). No alterations in cable properties or experimental recording were observed, and mEPSCs parameters from all groups were similarly correlated with series resistance, input resistance and cell capacitance (Figure S6) (Spruston et al., 1993). A role for 4E-BP2 deamidation is thus implied in the timing of excitatory postsynaptic signals independently of its effect on synaptic strength. Possible mechanistic explanations for this finding are addressed below.

Discussion

We present here the characterization of a developmentally patterned posttranslational modification of 4E-BP2 in the brain. Deamidation of two asparagines in 4E-BP2 enhances its binding to mTORC1 and reduces the kinetics of synaptic transmission. The genetic encoding of asparagines that are susceptible to deamidation appears to be selected for and may act as a ‘molecular clock’ to regulate important biological events (Robinson and Robinson, 1991; Robinson and Robinson, 2001). Therefore, the fact that the C-terminal, deamidation sequence is perfectly conserved in 4E-BP2 in mammals but not in lower organisms, many of which possess only a single 4E-BP gene (Figure S6), suggests a genetically-controlled link to regulation of higher brain function.

The interaction of deamidated 4E-BP2 with raptor is enhanced relative to the wild type form. Altered protein-protein interactions have also been demonstrated to be a consequence of deamidation of Bcl-X_L and fibronectin (Curnis et al., 2006; Deverman et al., 2002). 4E-BP2 deamidation therefore appears to have an auxiliary function in the TOS-dependent binding of 4E-BP2 to raptor. This is consistent with recent findings of an insufficiency of the 4E-BP1 TOS motif for efficient raptor-binding (Lee et al., 2008). Moreover, this finding suggests that negative charges in the C-terminal region of 4E-BPs, possibly including non-conserved phosphorylation sites in 4E-BP1 (Wang et al., 2003), may enhance this interaction.

Deamidated 4E-BP2 displays reduced affinity for eIF4E, a phenomenon which persists in conditions of impaired mTORC1 activity and is dependent on interaction with raptor.

Moreover, deamidated 4E-BP2 exhibited weak translational repression toward two reporter mRNAs that contain significant 5′UTR secondary structure (Figures 4G and 4H). In agreement with this, alterations in eIF4E levels selectively affect the translation of mRNAs with extensive secondary structure in the 5′ untranslated leader sequence (De Benedetti and Graff, 2004; Graff et al., 2007; Koromilas et al., 1992; Richter and Sonenberg, 2005). As 4E-BPs control the availability eIF4E for eIF4F complex formation, the impact of 4E-BP2 deamidation on translation may be limited to specific mRNAs harbouring structured 5′UTRs, as opposed to bulk mRNAs. Furthermore, our findings suggest that a function of 4E-BP2 deamidation may be to compensate for impaired upstream signalling that normally effects its phosphorylation. Our observation that the eIF4F complex displays remarkable stability despite dramatic reduction in mTORC1 activity during early brain development (Figure 5F) is consistent with this notion.

How might the interaction of deamidated 4E-BP2 with raptor lead to reduced binding to eIF4E? It is possible that raptor spatially sequesters 4E-BP2 away from eIF4E. This is conceivable in light of previous reports demonstrating 4E-BP-dependent nuclear accumulation of eIF4E upon inhibition of mTORC1 (Rong et al., 2008), and raptor-dependent perinuclear localization of mTOR following release from amino-acid deprivation (Sancak et al., 2008). Thus, putative partitioning of 4E-BP2 between eIF4E and raptor may favour interaction and co-localization with raptor at the expense of eIF4E upon deamidation. In neurons, such an effect could occur locally in dendrites as opposed to the cell body. It is also possible that enhanced phosphorylation of deamidated 4E-BP2 may occur at activated dendritic synapses, consistent with the previous detection by immunofluorescence of 4E-BP2 in dendritic puncta (Tang et al., 2002) and DHPG-induced 4E-BP2 phosphorylation (T37/T46) in the stratum radiatum (Banko et al., 2006). Yet, our inability to detect phosphorylated 4E-BP2 in the adult brain suggests that such local phosphorylation may be largely diluted in whole cell lysates.

Pyramidal 4E-BP2−/− neurons displayed enhancement in mEPSC amplitude, frequency, and charge transfer. Since the expression of wild type or deamidated 4E-BP2 in post-synaptic 4E-BP2−/− neurons abolished the increase in amplitude and frequency, predominantly post-synaptic changes, such as surface AMPA receptor expression, likely mediate these changes (Malinow and Malenka, 2002). In contrast, charge transfer was only partially repressed by expression of deamidated 4E-BP2 in 4E-BP2−/− neurons. Consistent with this finding, a salient feature of our electrophysiological analysis is that mEPSCs in neurons expressing deamidated 4E-BP2 exhibit slower rise and decay times, relative to controls. This could favour enhanced signal integration and, thus, plasticity. Importantly, mEPSCs have also been shown to influence neuronal firing, synaptic restructuring, and activation of postsynaptic signaling cascades (Carter and Regehr, 2002; McKinney et al., 1999; Murphy et al., 1994; Sharma and Vijayaraghavan, 2003).

How might deamidated 4E-BP2 influence mEPSC kinetics? One possibility is based on cable theory, which posits that the magnitude and kinetics of currents originating from distal synapses become attenuated to a greater extent, while approaching the cell body, than those more proximal to the soma (Bekkers and Stevens, 1996; Williams and Johnston, 1991). However, AMPA receptor-mediated mEPSC amplitudes are relatively independent of synapse location (Magee and Cook, 2000). Thus, deamidated 4E-BP2 might favour currents emanating from distal dendritic regions, whereas such spatial selectivity would not be expected with expression of the wild type protein. Indeed, we observed a near absence (< 5%) of fast mEPSCs upon expression of deamidated 4E-BP2. This is consistent with an efficient and selective repression of synaptic activity at synapses located proximally, whereas distally located “de-repressed” synapses remain intact. This would account for mEPSCs exhibiting slower kinetics. An alternative explanation is that the slower kinetics resulted from changes in cell cable properties or recording quality (Spruston et al., 1993). However this appears unlikely since series

resistance, input resistance and cell capacitance did not differ between neurons in all groups (Figure S6), thus suggesting that the slower kinetics arise from direct effects on mEPSCs. A third potential interpretation is that AMPA receptor channel gating is protracted. This could be due to alterations in the subunit composition of the tetrameric AMPA receptors (Jonas, 2000) or the relative expression of AMPAR-associated auxiliary proteins (Milstein and Nicoll, 2008), both of which are known to influence postsynaptic current kinetics. In particular, transmembrane AMPA receptor regulatory proteins (TARPs) (Milstein and Nicoll, 2008) and cornichons (Schwenk et al., 2009) interact with AMPA receptors and slow gating kinetics and increase charge transfer. However, TARPs tend to regulate decay kinetics and have only a small influence on rise times. Indeed, in small cerebellar granule cells, the affect of TARPs on activation kinetics (~0.5 ms) were less than those observed here (~1.5-2.0 ms) (Milstein et al., 2007). Thus, in large pyramidal neurons the rise times of mEPSCs are filtered by the cable properties of the neuron and do not reflect AMPA receptor gating kinetics. The observed effect on decay kinetics, however, were in the range (7 – 12 ms) of those observed by TARP modulation (Milstein et al., 2007) and are likely less affected by cable properties. Despite the above possibilities, the mechanism responsible for deamidated 4E-BP2-dependent slow mEPSCs and its importance for evoked synaptic transmission is presently unclear.

Recent work reported that mEPSCs block local dendritic translation to provide a rapid response to postsynaptic activity. Increased protein synthesis and synaptic efficacy homeostatically compensate for tonic inhibition of action potentials that is coupled to mEPSC blockade (Sutton et al., 2006; Sutton et al., 2007; Sutton et al., 2004). In acute measurements (30 minutes) however, we find larger and more frequent mEPSCs in the absence of a translation inhibitor, a context which engenders enhanced synaptic transmission (Figure 6A). The initial reports demonstrating a role for 4E-BP2 in synaptic plasticity found no change in basal synaptic function upon genetic deletion of 4E-BP2 in mice (Banko et al., 2006; Banko et al., 2005). Our finding of enhanced mEPSCs in 4E-BP2−/− organotypic slices is not at variance with this conclusion as our results are based on non-evoked spontaneous quantal events, whereas the observations of Banko et al. were induced by synaptic network stimulation. Thus, we have revealed a unique modification of 4E-BP2 in the brain and a function for it in synaptic activity.

Experimental Procedures

Cell Culture, Transfections, Alkaline and Phosphatase Treatments

For transfection of HEK293 or HEK293E cells, 1 million cells/well were seeded in six-well culture plates and 24 hours later were transfected for 3-5 hours using Lipofectamine/Plus reagents (Invitrogen). Cells were harvested 24 hours post-transfection. Alkaline treatments on cell extracts were performed as previously described (Deverman et al., 2002). Alkalinization of recombinant 4E-BP2 protein was at 37°C in 0.15M Tris-HCl, pH 7.0 or 10.0. For phosphatase treatments, tissues were homogenized in 1X λ phosphatase buffer containing 0.5 μg/mL leupetin and 1mM PMSF. Lysates (90μl) were incubated with 9μl of λ phosphatase at 30°C for 45 minutes.

Far Western Assay

Flag-HMK-eIF4E probe labelling, purification and Far Western blotting has been described elsewhere (Gingras et al., 1996; Pause et al., 1994).

Immunoprecipitation and m^7GDP Pull-down

For immunoprecipitation, lysates (200μg) were mixed with Myc antibody for 1.5 hours at 4° C, followed by 1 hour incubation with 25μl of Protein G Sepharose (GE Healthcare). For m^7GDP pull-downs, lysates were mixed with 30μl of m^7GDP-agarose for 1.5 hours at 4°C. In either case, the resins were washed 4 times and proteins were eluted with 2X sample buffer.

Mass Spectrometry Analysis of *In Vitro* Deamidated Recombinant 4E-BP2

Analysis of resolved 4E-BP2 species, obtained from alkaline treatment, was with a ThermoFinnigan LTQ-Orbitrap hybrid mass spectrometer. Searches were conducted using X! Tandem, with comparison to the IPI human database. Spectra corresponding to the peptide *VEVNNLNNLNNHDR* were manually inspected for the proper assignment of the deamidated species.

Luciferase Assays

Co-transfection of MEFs with reporter plasmids and analysis of luciferase activity was performed as previously described (Colina et al., 2008). Free energies of formation of mRNA secondary structures were predicted with Mfold (Zuker, 2003). Differences between group means obtained from independent experiments were considered significant at $p < 0.05$ by Student's t-test.

Primary Neuron Culture, Transfection, Image Analysis

Hippocampal neuron cultures were prepared as previously described (Goslin et al., 1988).Ten days after plating, neurons were co-transfected with 2μg of 4E-BP2 expression plasmid and 1.5μg of $5'_{myr}$dYFP3′ reporter plasmid using Lipofectamine 2000 (Invitrogen) and returned to conditioned medium. Two days later cells were fixed and processed for immunofluorescence using 4E-BP2 antibody (Cell Signaling), as described elsewhere (Lebeau et al., 2008). Images of co-transfected neurons were acquired on an Olympus FV300 confocal microscope using a 40X PlanFluor 0.75 numerical aperture objective. Analysis of dYFP fluorescence from z-compressed stacks was with Image J (NIH). Mean fluorescence for each group was reported and statistical significance was determined by Student's t-test.

Organotypic hippocampal slice cultures, transfections, and electrophysiology

Hippocampal slice cultures were prepared and biolistically transfected as previously described (Bourdeau et al., 2007; Lebeau et al., 2008; Ran et al., 2009). Whole cell recordings were obtained from transfected CA1 pyramidal neurons (Lebeau et al., 2008) in submerged slice culture conditions (Ran et al., 2009) and mEPSC recording acquisition and analysis were performed with pClamp9 software (Molecular Devices) as previously described (Ran et al., 2009). mEPSC parameters were compared between groups using Kolmogorov-Smirnov tests. A one-way ANOVA and Bonferroni post-hoc tests were used to compare passive membrane properties. Data represent means ± SEM, unless otherwise mentioned, and statistical significance was set at $p < 0.05$.

Highlights

- 4E-BP2 undergoes asparagine deamidation uniquely in the brain
- 4E-BP2 deamidation enhances its association with raptor and reduces eIF4E-binding
- 4E-BP2 deamidation is developmentally regulated
- Deamidated 4E-BP2 slows excitatory Schaffer collateral synaptic transmission

Supplementary Material

Refer to Web version on PubMed Central for supplementary material.

Acknowledgments

We thank C. Lister and A. Sylvestre for excellent technical assistance and J. Pelletier, M. Livingstone, I. Topisirovic, and M.R. Fabian for helpful discussions. We thank B. Lane and the Harvard Microchemistry and Proteomics Analysis Facility for mass spectrometry analysis. pcDNA3.1-5′$_{myr}$dGFP3′ (CamKIIα) was a kind gift from E.M. Schuman. This work was supported by a Team grant from the Canadian Institutes of Health Research to N.S. and J.-C.L. and a Howard Hughes Medical Institute (HHMI) grant to N.S. who is an HHMI International Scholar. M.B. was the recipient of a Postgraduate Doctoral Scholarship from the Natural Sciences and Engineering Research Council of Canada.

References

Aakalu G, Smith WB, Nguyen N, Jiang C, Schuman EM. Dynamic visualization of local protein synthesis in hippocampal neurons. Neuron 2001;30:489–502. [PubMed: 11395009]

Banko JL, Hou L, Poulin F, Sonenberg N, Klann E. Regulation of eukaryotic initiation factor 4E by converging signaling pathways during metabotropic glutamate receptor-dependent long-term depression. J Neurosci 2006;26:2167–2173. [PubMed: 16495443]

Banko JL, Merhav M, Stern E, Sonenberg N, Rosenblum K, Klann E. Behavioral alterations in mice lacking the translation repressor 4E-BP2. Neurobiol Learn Mem 2007;87:248–256. [PubMed: 17029989]

Banko JL, Poulin F, Hou L, DeMaria CT, Sonenberg N, Klann E. The translation repressor 4E-BP2 is critical for eIF4F complex formation, synaptic plasticity, and memory in the hippocampus. J Neurosci 2005;25:9581–9590. [PubMed: 16237163]

Bekkers JM, Stevens CF. Cable properties of cultured hippocampal neurons determined from sucrose-evoked miniature EPSCs. J Neurophysiol 1996;75:1250–1255. [PubMed: 8867133]

Bourdeau ML, Morin F, Laurent CE, Azzi M, Lacaille JC. Kv4.3-mediated A-type K+ currents underlie rhythmic activity in hippocampal interneurons. J Neurosci 2007;27:1942–1953. [PubMed: 17314290]

Cammalleri M, Lutjens R, Berton F, King AR, Simpson C, Francesconi W, Sanna PP. Time-restricted role for dendritic activation of the mTOR-p70S6K pathway in the induction of late-phase long-term potentiation in the CA1. Proc Natl Acad Sci U S A 2003;100:14368–14373. [PubMed: 14623952]

Carter AG, Regehr WG. Quantal events shape cerebellar interneuron firing. Nat Neurosci 2002;5:1309–1318. [PubMed: 12411959]

Choi KM, McMahon LP, Lawrence JC Jr. Two motifs in the translational repressor PHAS-I required for efficient phosphorylation by mammalian target of rapamycin and for recognition by raptor. J Biol Chem 2003;278:19667–19673. [PubMed: 12665511]

Colina R, Costa-Mattioli M, Dowling RJ, Jaramillo M, Tai LH, Breitbach CJ, Martineau Y, Larsson O, Rong L, Svitkin YV, et al. Translational control of the innate immune response through IRF-7. Nature 2008;452:323–328. [PubMed: 18272964]

Curnis F, Longhi R, Crippa L, Cattaneo A, Dondossola E, Bachi A, Corti A. Spontaneous formation of L-isoaspartate and gain of function in fibronectin. J Biol Chem 2006;281:36466–36476. [PubMed: 17015452]

De Benedetti A, Graff JR. eIF-4E expression and its role in malignancies and metastases. Oncogene 2004;23:3189–3199. [PubMed: 15094768]

Deverman BE, Cook BL, Manson SR, Niederhoff RA, Langer EM, Rosova I, Kulans LA, Fu X, Weinberg JS, Heinecke JW, et al. Bcl-xL deamidation is a critical switch in the regulation of the response to DNA damage. Cell 2002;111:51–62. [PubMed: 12372300]

Eguchi S, Tokunaga C, Hidayat S, Oshiro N, Yoshino K, Kikkawa U, Yonezawa K. Different roles for the TOS and RAIP motifs of the translational regulator protein 4E-BP1 in the association with raptor and phosphorylation by mTOR in the regulation of cell size. Genes Cells 2006;11:757–766. [PubMed: 16824195]

Ehninger D, Han S, Shilyansky C, Zhou Y, Li W, Kwiatkowski DJ, Ramesh V, Silva AJ. Reversal of learning deficits in a Tsc2+/− mouse model of tuberous sclerosis. Nat Med 2008;14:843–848. [PubMed: 18568033]

Gingras AC, Gygi SP, Raught B, Polakiewicz RD, Abraham RT, Hoekstra MF, Aebersold R, Sonenberg N. Regulation of 4E-BP1 phosphorylation: a novel two-step mechanism. Genes Dev 1999a;13:1422–1437. [PubMed: 10364159]

Gingras AC, Raught B, Gygi SP, Niedzwiecka A, Miron M, Burley SK, Polakiewicz RD, Wyslouch-Cieszynska A, Aebersold R, Sonenberg N. Hierarchical phosphorylation of the translation inhibitor 4E-BP1. Genes Dev 2001a;15:2852–2864. [PubMed: 11691836]

Gingras AC, Raught B, Sonenberg N. eIF4 initiation factors: effectors of mRNA recruitment to ribosomes and regulators of translation. Annu Rev Biochem 1999b;68:913–963. [PubMed: 10872469]

Gingras AC, Raught B, Sonenberg N. Regulation of translation initiation by FRAP/mTOR. Genes Dev 2001b;15:807–826. [PubMed: 11297505]

Gingras AC, Svitkin Y, Belsham GJ, Pause A, Sonenberg N. Activation of the translational suppressor 4E-BP1 following infection with encephalomyocarditis virus and poliovirus. Proc Natl Acad Sci U S A 1996;93:5578–5583. [PubMed: 8643618]

Gobert D, Topolnik L, Azzi M, Huang L, Badeaux F, Desgroseillers L, Sossin WS, Lacaille JC. Forskolin induction of late-LTP and up-regulation of 5′ TOP mRNAs translation via mTOR, ERK, and PI3K in hippocampal pyramidal cells. J Neurochem 2008;106:1160–1174. [PubMed: 18466337]

Gong R, Park CS, Abbassi NR, Tang SJ. Roles of glutamate receptors and the mammalian target of rapamycin (mTOR) signaling pathway in activity-dependent dendritic protein synthesis in hippocampal neurons. J Biol Chem 2006;281:18802–18815. [PubMed: 16651266]

Goslin K, Schreyer DJ, Skene JH, Banker G. Development of neuronal polarity: GAP-43 distinguishes axonal from dendritic growth cones. Nature 1988;336:672–674. [PubMed: 3059197]

Graff JR, Konicek BW, Vincent TM, Lynch RL, Monteith D, Weir SN, Schwier P, Capen A, Goode RL, Dowless MS, et al. Therapeutic suppression of translation initiation factor eIF4E expression reduces tumor growth without toxicity. J Clin Invest 2007;117:2638–2648. [PubMed: 17786246]

Haghighat A, Mader S, Pause A, Sonenberg N. Repression of cap-dependent translation by 4E-binding protein 1: competition with p220 for binding to eukaryotic initiation factor-4E. EMBO J 1995;14:5701–5709. [PubMed: 8521827]

Jaworski J, Spangler S, Seeburg DP, Hoogenraad CC, Sheng M. Control of dendritic arborization by the phosphoinositide-3′-kinase-Akt-mammalian target of rapamycin pathway. J Neurosci 2005;25:11300–11312. [PubMed: 16339025]

Jonas P. The Time Course of Signaling at Central Glutamatergic Synapses. News Physiol Sci 2000;15:83–89. [PubMed: 11390884]

Kelleher RJ 3rd, Govindarajan A, Jung HY, Kang H, Tonegawa S. Translational control by MAPK signaling in long-term synaptic plasticity and memory. Cell 2004;116:467–479. [PubMed: 15016380]

Koromilas AE, Lazaris-Karatzas A, Sonenberg N. mRNAs containing extensive secondary structure in their 5′ non-coding region translate efficiently in cells overexpressing initiation factor eIF-4E. EMBO J 1992;11:4153–4158. [PubMed: 1396596]

Kumar V, Zhang MX, Swank MW, Kunz J, Wu GY. Regulation of dendritic morphogenesis by Ras-PI3K-Akt-mTOR and Ras-MAPK signaling pathways. J Neurosci 2005;25:11288–11299. [PubMed: 16339024]

Lebeau G, Maher-Laporte M, Topolnik L, Laurent CE, Sossin W, Desgroseillers L, Lacaille JC. Staufen1 regulation of protein synthesis-dependent long-term potentiation and synaptic function in hippocampal pyramidal cells. Mol Cell Biol 2008;28:2896–2907. [PubMed: 18316402]

Lee VH, Healy T, Fonseca BD, Hayashi A, Proud CG. Analysis of the regulatory motifs in eukaryotic initiation factor 4E-binding protein 1. FEBS J 2008;275:2185–2199. [PubMed: 18384376]

Lin TA, Kong X, Haystead TA, Pause A, Belsham G, Sonenberg N, Lawrence JC Jr. PHAS-I as a link between mitogen-activated protein kinase and translation initiation. Science 1994;266:653–656. [PubMed: 7939721]

Lisman JE, Raghavachari S, Tsien RW. The sequence of events that underlie quantal transmission at central glutamatergic synapses. Nat Rev Neurosci 2007;8:597–609. [PubMed: 17637801]

Ma XM, Blenis J. Molecular mechanisms of mTOR-mediated translational control. Nat Rev Mol Cell Biol 2009;10:307–318. [PubMed: 19339977]

Mader S, Lee H, Pause A, Sonenberg N. The translation initiation factor eIF-4E binds to a common motif shared by the translation factor eIF-4 gamma and the translational repressors 4E-binding proteins. Mol Cell Biol 1995;15:4990–4997. [PubMed: 7651417]

Magee JC, Cook EP. Somatic EPSP amplitude is independent of synapse location in hippocampal pyramidal neurons. Nat Neurosci 2000;3:895–903. [PubMed: 10966620]

Malinow R, Malenka RC. AMPA receptor trafficking and synaptic plasticity. Annu Rev Neurosci 2002;25:103–126. [PubMed: 12052905]

Marcotrigiano J, Gingras AC, Sonenberg N, Burley SK. Cap-dependent translation initiation in eukaryotes is regulated by a molecular mimic of eIF4G. Mol Cell 1999;3:707–716. [PubMed: 10394359]

McKinney RA, Capogna M, Durr R, Gahwiler BH, Thompson SM. Miniature synaptic events maintain dendritic spines via AMPA receptor activation. Nat Neurosci 1999;2:44–49. [PubMed: 10195179]

Milstein AD, Nicoll RA. Regulation of AMPA receptor gating and pharmacology by TARP auxiliary subunits. Trends Pharmacol Sci 2008;29:333–339. [PubMed: 18514334]

Milstein AD, Zhou W, Karimzadegan S, Bredt DS, Nicoll RA. TARP subtypes differentially and dose-dependently control synaptic AMPA receptor gating. Neuron 2007;55:905–918. [PubMed: 17880894]

Mothe-Satney I, Yang D, Fadden P, Haystead TA, Lawrence JC Jr. Multiple mechanisms control phosphorylation of PHAS-I in five (S/T)P sites that govern translational repression. Mol Cell Biol 2000;20:3558–3567. [PubMed: 10779345]

Murphy TH, Blatter LA, Bhat RV, Fiore RS, Wier WG, Baraban JM. Differential regulation of calcium/calmodulin-dependent protein kinase II and p42 MAP kinase activity by synaptic transmission. J Neurosci 1994;14:1320–1331. [PubMed: 8120627]

Nojima H, Tokunaga C, Eguchi S, Oshiro N, Hidayat S, Yoshino K, Hara K, Tanaka N, Avruch J, Yonezawa K. The mammalian target of rapamycin (mTOR) partner, raptor, binds the mTOR substrates p70 S6 kinase and 4E-BP1 through their TOR signaling (TOS) motif. J Biol Chem 2003;278:15461–15464. [PubMed: 12604610]

Park KK, Liu K, Hu Y, Smith PD, Wang C, Cai B, Xu B, Connolly L, Kramvis I, Sahin M, He Z. Promoting axon regeneration in the adult CNS by modulation of the PTEN/mTOR pathway. Science 2008;322:963–966. [PubMed: 18988856]

Parsons RG, Gafford GM, Helmstetter FJ. Translational control via the mammalian target of rapamycin pathway is critical for the formation and stability of long-term fear memory in amygdala neurons. J Neurosci 2006;26:12977–12983. [PubMed: 17167087]

Pause A, Belsham GJ, Gingras AC, Donze O, Lin TA, Lawrence JC Jr. Sonenberg N. Insulin-dependent stimulation of protein synthesis by phosphorylation of a regulator of 5′-cap function. Nature 1994;371:762–767. [PubMed: 7935836]

Pestova, TV.; Lorsch, JR.; Hellen, CUT. The Mechanism of Translation Initiation in Eukaryotes. In: Mathews, MB.; Sonenberg, N.; Hershey, JWB., editors. Translational Control in Biology and Medicine. Cold Spring Harbor Laboratory Press; Cold Spring Harbor, NY: 2007. p. 87-128.

Proud CG. mTORC1 signalling and mRNA translation. Biochem Soc Trans 2009;37:227–231. [PubMed: 19143637]

Ran I, Laplante I, Bourgeois C, Pepin J, Lacaille P, Costa-Mattioli M, Pelletier J, Sonenberg N, Lacaille JC. Persistent transcription- and translation-dependent long-term potentiation induced by mGluR1 in hippocampal interneurons. J Neurosci 2009;29:5605–5615. [PubMed: 19403827]

Richter JD, Sonenberg N. Regulation of cap-dependent translation by eIF4E inhibitory proteins. Nature 2005;433:477–480. [PubMed: 15690031]

Robinson AB, Robinson LR. Distribution of glutamine and asparagine residues and their near neighbors in peptides and proteins. Proc Natl Acad Sci U S A 1991;88:8880–8884. [PubMed: 1924347]

Robinson AB, Rudd CJ. Deamidation of glutaminyl and asparaginyl residues in peptides and proteins. Curr Top Cell Regul 1974;8:247–295. [PubMed: 4371091]

Robinson AB, Scotchler JW, McKerrow JH. Rates of nonenzymatic deamidation of glutaminyl and asparaginyl residues in pentapeptides. J Am Chem Soc 1973;95:8156–8159. [PubMed: 4762548]

Robinson NE, Robinson AB. Molecular clocks. Proc Natl Acad Sci U S A 2001;98:944–949. [PubMed: 11158575]

Rong L, Livingstone M, Sukarieh R, Petroulakis E, Gingras AC, Crosby K, Smith B, Polakiewicz RD, Pelletier J, Ferraiuolo MA, Sonenberg N. Control of eIF4E cellular localization by eIF4E-binding proteins, 4E-BPs. RNA 2008;14:1318–1327. [PubMed: 18515545]

Sancak Y, Peterson TR, Shaul YD, Lindquist RA, Thoreen CC, Bar-Peled L, Sabatini DM. The Rag GTPases bind raptor and mediate amino acid signaling to mTORC1. Science 2008;320:1496–1501. [PubMed: 18497260]

Sancak Y, Sabatini DM. Rag proteins regulate amino-acid-induced mTORC1 signalling. Biochem Soc Trans 2009;37:289–290. [PubMed: 19143648]

Sarbassov DD, Ali SM, Sabatini DM. Growing roles for the mTOR pathway. Curr Opin Cell Biol 2005;17:596–603. [PubMed: 16226444]

Schalm SS, Fingar DC, Sabatini DM, Blenis J. TOS motif-mediated raptor binding regulates 4E-BP1 multisite phosphorylation and function. Curr Biol 2003;13:797–806. [PubMed: 12747827]

Schwenk J, Harmel N, Zolles G, Bildl W, Kulik A, Heimrich B, Chisaka O, Jonas P, Schulte U, Fakler B, Klocker N. Functional proteomics identify cornichon proteins as auxiliary subunits of AMPA receptors. Science 2009;323:1313–1319. [PubMed: 19265014]

Sharma G, Vijayaraghavan S. Modulation of presynaptic store calcium induces release of glutamate and postsynaptic firing. Neuron 2003;38:929–939. [PubMed: 12818178]

Spruston N, Jaffe DB, Williams SH, Johnston D. Voltage- and space-clamp errors associated with the measurement of electrotonically remote synaptic events. J Neurophysiol 1993;70:781–802. [PubMed: 8410172]

Sutton MA, Ito HT, Cressy P, Kempf C, Woo JC, Schuman EM. Miniature neurotransmission stabilizes synaptic function via tonic suppression of local dendritic protein synthesis. Cell 2006;125:785–799. [PubMed: 16713568]

Sutton MA, Taylor AM, Ito HT, Pham A, Schuman EM. Postsynaptic decoding of neural activity: eEF2 as a biochemical sensor coupling miniature synaptic transmission to local protein synthesis. Neuron 2007;55:648–661. [PubMed: 17698016]

Sutton MA, Wall NR, Aakalu GN, Schuman EM. Regulation of dendritic protein synthesis by miniature synaptic events. Science 2004;304:1979–1983. [PubMed: 15218151]

Takei N, Inamura N, Kawamura M, Namba H, Hara K, Yonezawa K, Nawa H. Brain-derived neurotrophic factor induces mammalian target of rapamycin-dependent local activation of translation machinery and protein synthesis in neuronal dendrites. J Neurosci 2004;24:9760–9769. [PubMed: 15525761]

Takei N, Kawamura M, Hara K, Yonezawa K, Nawa H. Brain-derived neurotrophic factor enhances neuronal translation by activating multiple initiation processes: comparison with the effects of insulin. J Biol Chem 2001;276:42818–42825. [PubMed: 11551908]

Tang SJ, Reis G, Kang H, Gingras AC, Sonenberg N, Schuman EM. A rapamycin-sensitive signaling pathway contributes to long-term synaptic plasticity in the hippocampus. Proc Natl Acad Sci U S A 2002;99:467–472. [PubMed: 11756682]

Tsokas P, Grace EA, Chan P, Ma T, Sealfon SC, Iyengar R, Landau EM, Blitzer RD. Local protein synthesis mediates a rapid increase in dendritic elongation factor 1A after induction of late long-term potentiation. J Neurosci 2005;25:5833–5843. [PubMed: 15958750]

Tsukiyama-Kohara K, Poulin F, Kohara M, DeMaria CT, Cheng A, Wu Z, Gingras AC, Katsume A, Elchebly M, Spiegelman BM, et al. Adipose tissue reduction in mice lacking the translational inhibitor 4E-BP1. Nat Med 2001;7:1128–1132. [PubMed: 11590436]

Wang L, Rhodes CJ, Lawrence JC Jr. Activation of mammalian target of rapamycin (mTOR) by insulin is associated with stimulation of 4EBP1 binding to dimeric mTOR complex 1. J Biol Chem 2006;281:24293–24303. [PubMed: 16798736]

Wang X, Li W, Parra JL, Beugnet A, Proud CG. The C terminus of initiation factor 4E-binding protein 1 contains multiple regulatory features that influence its function and phosphorylation. Mol Cell Biol 2003;23:1546–1557. [PubMed: 12588975]

Williams SH, Johnston D. Kinetic properties of two anatomically distinct excitatory synapses in hippocampal CA3 pyramidal neurons. J Neurophysiol 1991;66:1010–1020. [PubMed: 1661323]

Wullschleger S, Loewith R, Hall MN. TOR signaling in growth and metabolism. Cell 2006;124:471–484. [PubMed: 16469695]

Xie M, Schowen RL. Secondary structure and protein deamidation. J Pharm Sci 1999;88:8–13. [PubMed: 9874696]

Yonezawa K, Yoshino KI, Tokunaga C, Hara K. Kinase activities associated with mTOR. Curr Top Microbiol Immunol 2004;279:271–282. [PubMed: 14560963]

Zuker M. Mfold web server for nucleic acid folding and hybridization prediction. Nucleic Acids Res 2003;31:3406–3415. [PubMed: 12824337]

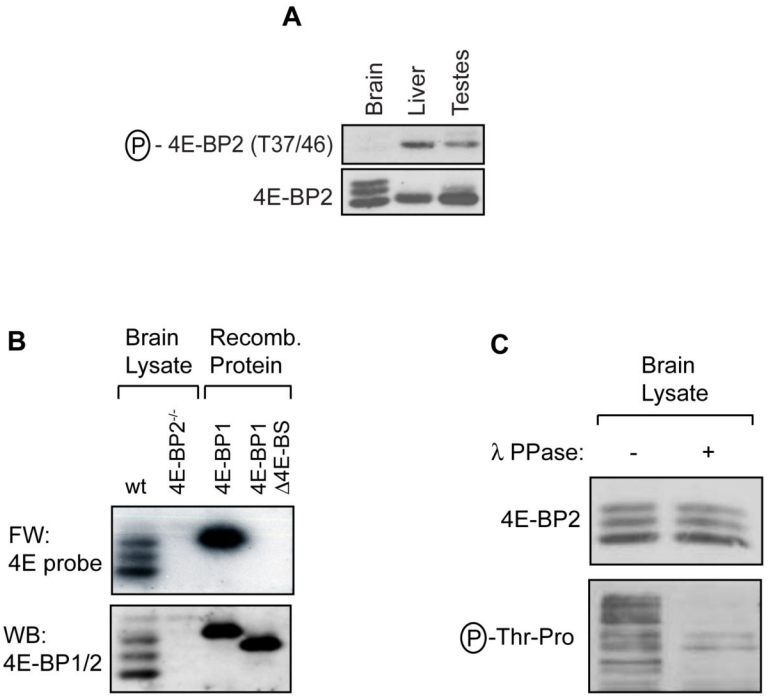

Figure 1. Slow-migrating forms of 4E-BP2 in the adult brain are independent of phosphorylation

(A) Reduced phosphorylation and a slow-migrating 4E-BP2 form are unique to the brain. Mouse tissue lysates (3 months) were analyzed by Western blotting (15% SDS-PAGE). (B) Far Western binding of eIF4E to 4E-BP2 from brain. Brain lysates were resolved and probed on a nitrocellulose membrane with radiolabeled FLAG-HMK-eIF4E protein. Recombinant 4E-BP1 and a variant lacking the eIF4E-binding site (Δ51-63) control for probe specificity. Western blotting was with antibody #11211. (C) 4E-BP2 from mouse brain is insensitive to phosphatase treatment. Brain lysates were incubated with λ phosphatase followed by Western blotting. phospho-Thr-Pro motif antibody demonstrates phosphatase efficacy (lower panel). See also Figure S1.

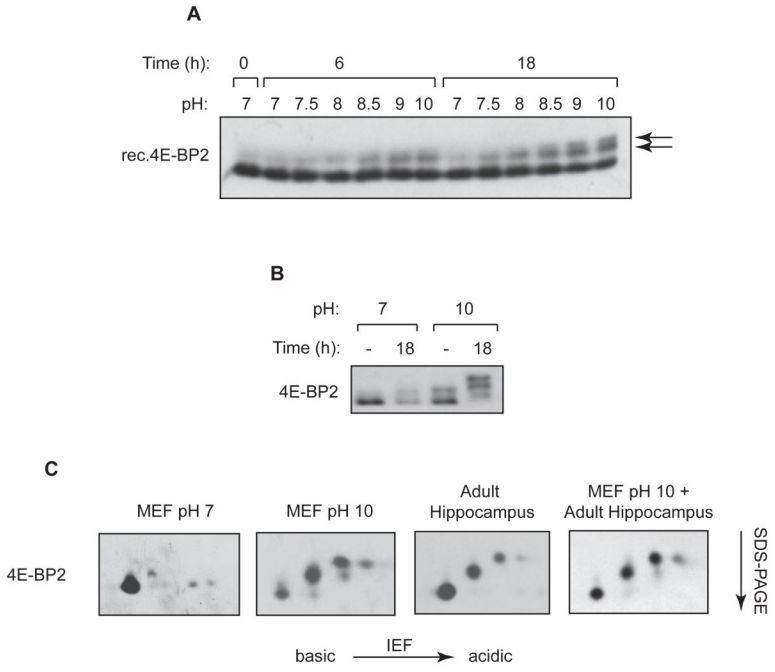

Figure 2. 4E-BP2 is susceptible to asparagine deamidation in the mammalian brain

(A) Deamidation of recombinant 4E-BP2 at high pH. Recombinant 4E-BP2 was incubated in 0.15M Tris-HCl at the indicated pH and times, followed by Western blotting. Arrow heads indicate deamidated forms of 4E-BP2. (B) Deamidation of 4E-BP2 in cell lysates. MEFs were starved of serum for 24 hours, followed by one hour in PBS. Cells were lysed at the indicated pH and extracts were incubated for 18 hours. (C) 4E-BP2 deamidation caused by alkaline treatment or occurring spontaneously in hippocampus exhibits identical migration pattern in two-dimensional isoelectric focusing/SDS-PAGE (IEF/SDS-PAGE). Alkaline-treated MEF or untreated hippocampal lysates were analysed (panels 1-3). In panel 4, a 1:1 mixture of pH 10-treated MEF and hippocampal lysates was analysed. See also Figure S2.

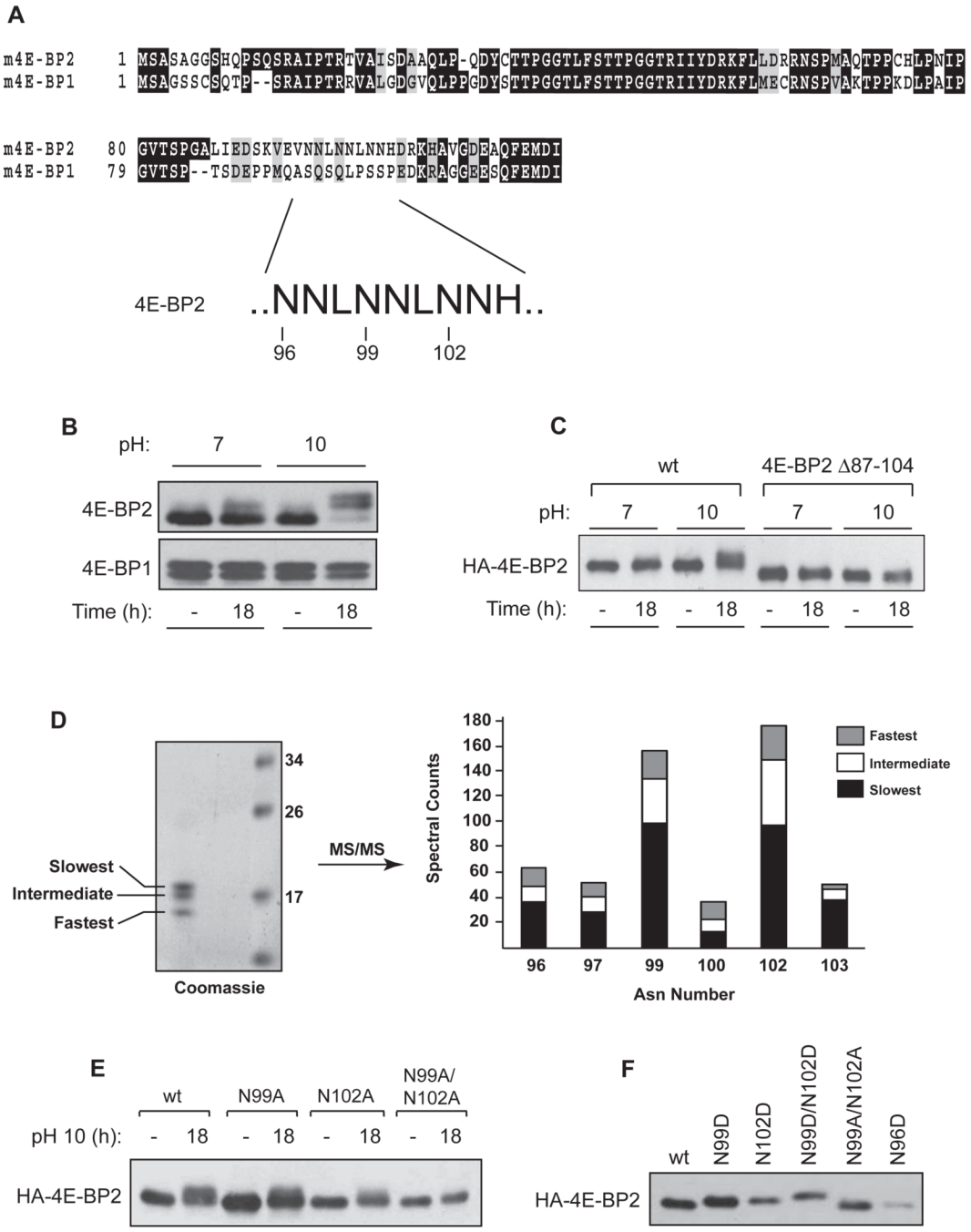

Figure 3. Deamidation of 4E-BP2 occurs on asparagines 99 and 102

(A) Amino acid sequence alignment of murine 4E-BP2 and 4E-BP1. Inset shows the asparagine-rich sequence of 4E-BP2. (B) 4E-BP2 is sensitive to alkaline-induced deamidation. MEFs were lysed and incubated as in (Figure 2B). (C) A 4E-BP2 variant lacking the asparagine-rich sequence is resistant to deamidation. HEK293E cells were transfected with N-terminal 3HA-tagged 4E-BP2 or a variant lacking residues 87-104. Post-transfection (24 hours) cells were lysed at pH 7 or 10 and incubated as indicated. (D) Asn99 and Asn102 are favoured for deamidation. Purified, recombinant 4E-BP2 protein was *in vitro* deamidated at pH 10 for 24h, resolved by SDS-PAGE (10-20%), and stained (left panel). Excised bands were analysed by LC-MS/MS (right). (E) Mutation of both Asn99 and Asn102 to alanines precludes alkaline-

induced deamidation. HEK293E cells were transfected and treated as in (C). (F) Mutation of Asn99 and Asn102 to aspartates retards 4E-BP2 migration. Cells were transfected as in (E). See also Figure S3.

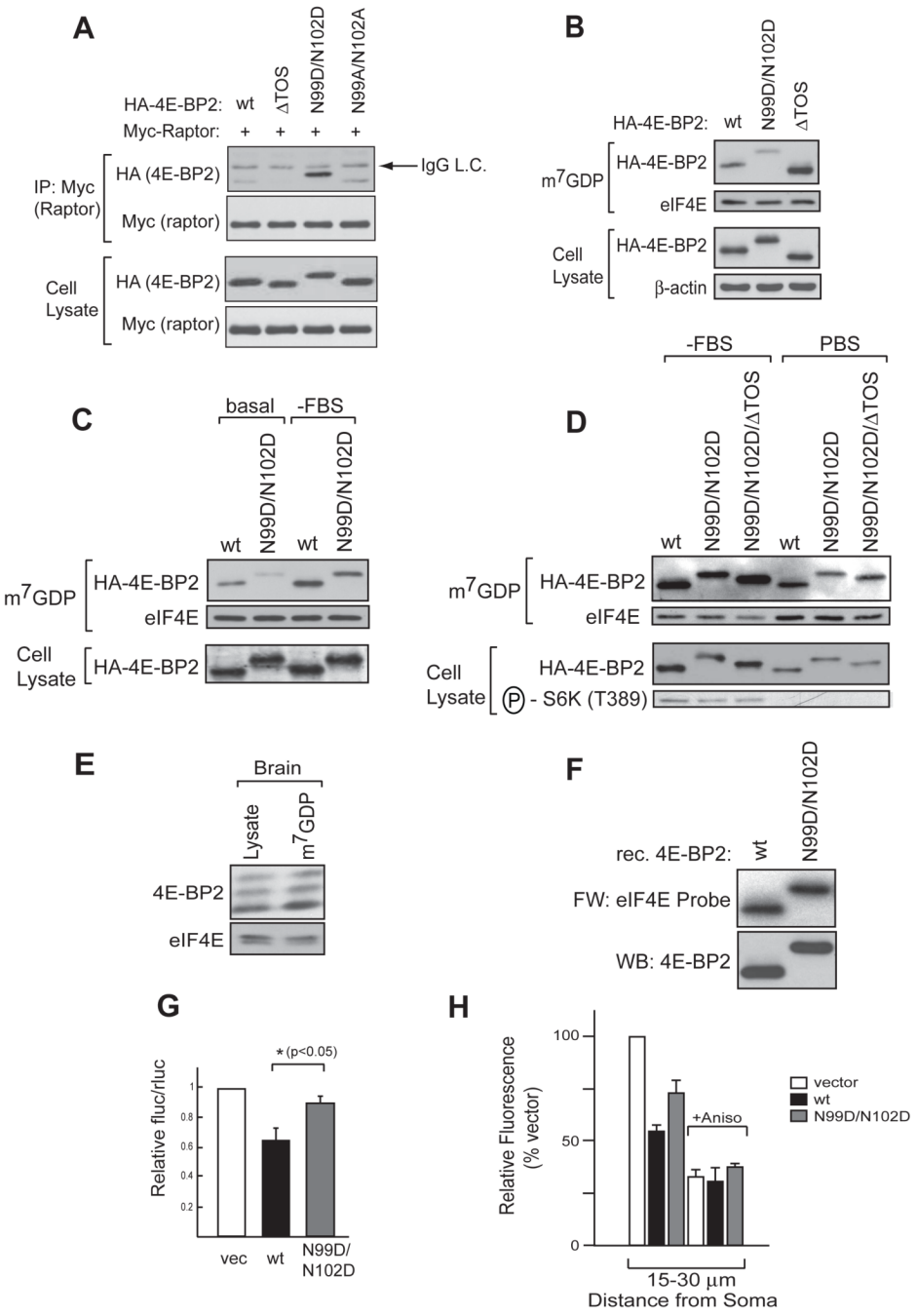

Figure 4. Deamidated 4E-BP2 exhibits increased raptor-interaction, reduced association to eIF4E and attenuated translational repression

(A) Deamidated 4E-BP2 exhibits enhanced affinity for raptor. HEK293 cells were co-transfected with Myc-tagged raptor and 3HA-tagged 4E-BP2. Anti-Myc immunoprecipitation was performed on lysates 24 hours later, followed by Western blotting (7-15% SDS-PAGE). (B) Deamidated 4E-BP2 is weakly associated to eIF4E in cells grown in complete medium. Lysates were incubated with m^7GDP agarose and bound proteins were analyzed by Western blotting. (C and D) Deamidated 4E-BP2 is more weakly associated to eIF4E in the absence of serum or nutrients. Cells were starved of serum for 24 hours (C) or incubated in D-PBS for 1 hour (D) followed by m^7GDP pulldown. (E) m^7GDP pulldowns from brain lysates were

performed as in (B). (F) Deamidation of 4E-BP2 does not affect eIF4E-binding in the absence of raptor. Far Western blotting was performed as in Figure 1C against recombinant proteins. (G and H) Deamidated 4E-BP2 weakly inhibits translation. 4E-BP1/4E-BP2 null MEFs were co-transfected with 4E-BP2 together with IRF7-Firefly Luciferase and Renilla luciferase plasmids (G) or cultured neurons were co-transfected with 4E-BP2 plasmids and a reporter encoding $_{myr}$dYFP flanked by the 5′ and 3′ UTRs of CamKIIα. MEFs in (G) were harvested 24 hours post-transfection and luciferase activity was measured (data are means ± SEM, with statistical significance set at $p < 0.05$). Cultured neurons in (H) were transfected 10 days after plating and two days later images of YFP-expressing neurons were acquired (N=9-12 cells; bars represent means ± SEM and in all cases, except amongst anisomycin treatments, means are different at $p < 0.05$ by Student's t-test). 4E-BP2 expression was determined by immunofluorescence and no differences between wild type and deamidated 4E-BP2 expression was observed in proximal dendrites (not shown). See also Figure S4.

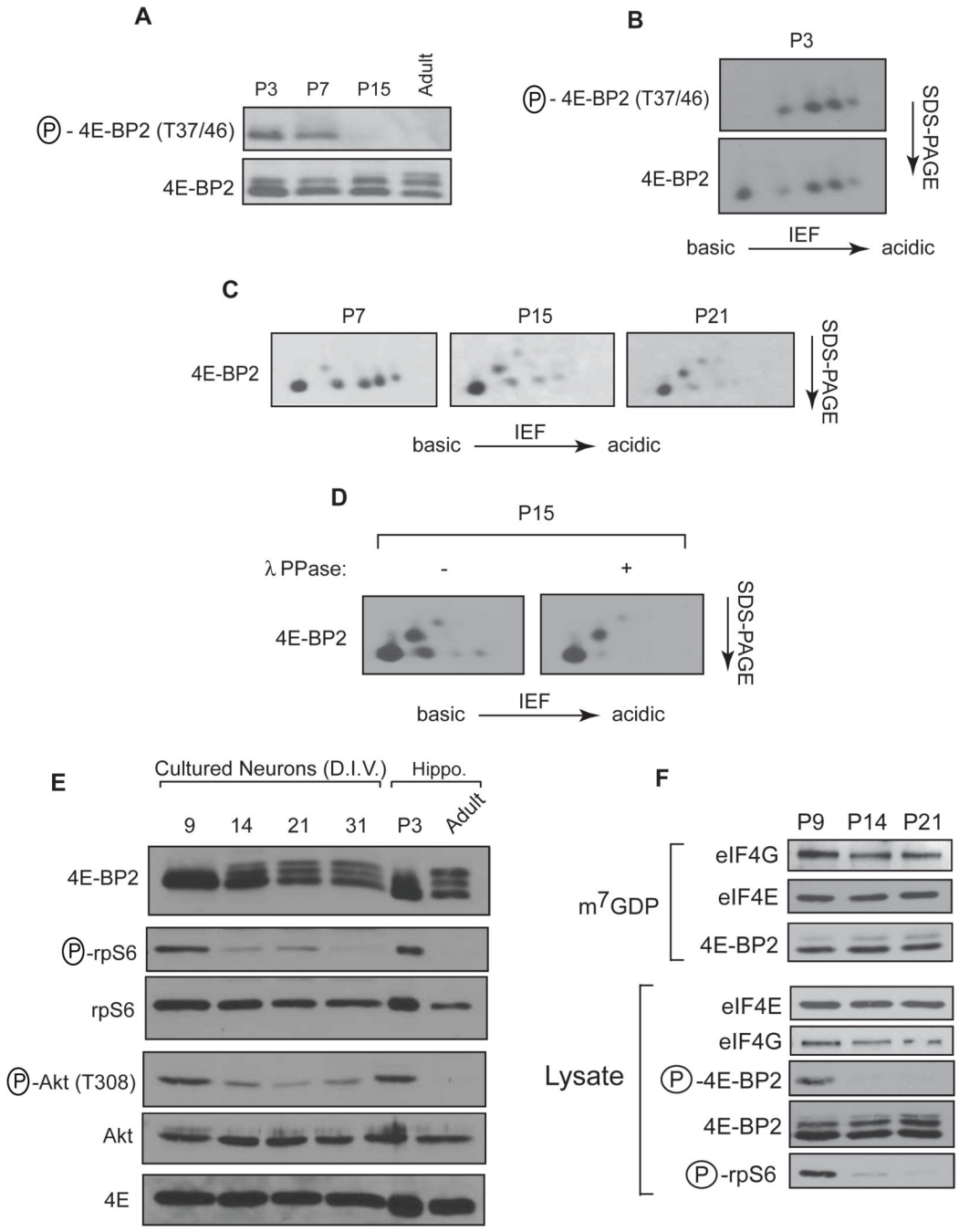

Figure 5. Deamidation of 4E-BP2 occurs during early postnatal brain development, concomitant with reduced PI3K-Akt-mTOR signaling

(A) Western blot analysis on hippocampal extracts (30μg each) from several postnatal (P) days compared with adult. (B) IEF/SDS-PAGE analysis of P3 hippocampal extract. (C) IEF/SDS-PAGE analysis of hippocampal extracts from indicated postnatal days. (D) Phosphatase treatment of P15 hippocampal extract. (E) SDS-PAGE analysis of lysates from dissociated hippocampal neuron cultures or brain from indicated days. (F) Analysis of associated eIF4E-binding proteins during hippocampal neuron development by m^7GDP precipitation. See also Figure S5.

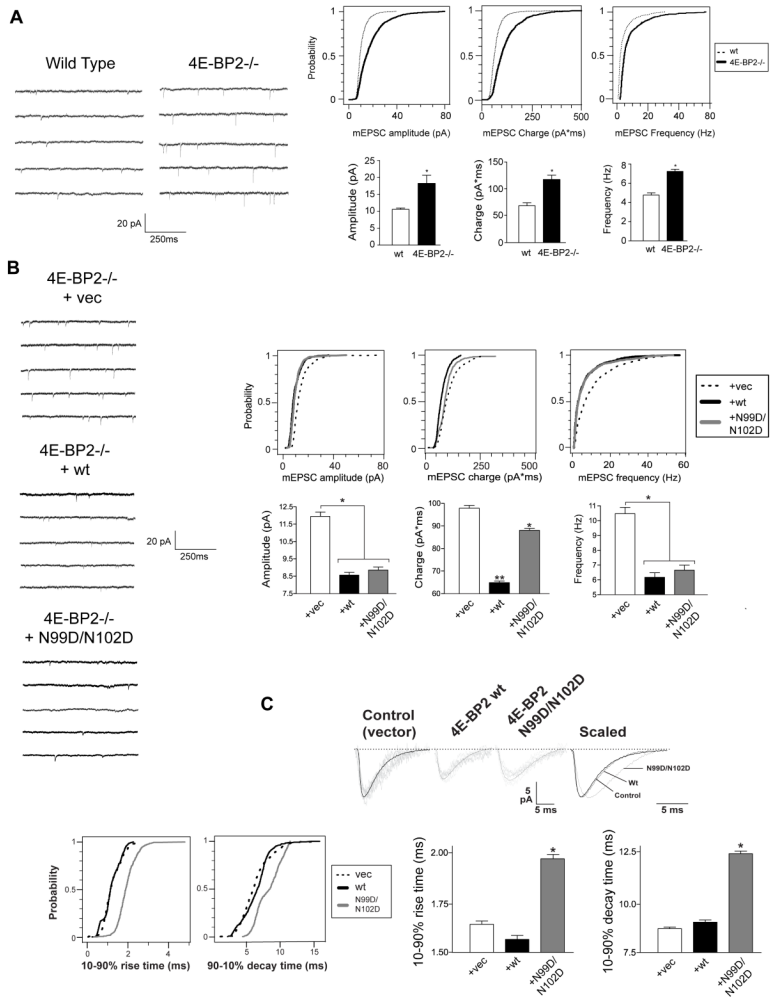

Figure 6. Expression of deamidated 4E-BP2 in 4E-BP2−/− neurons reduces elevated excitatory synaptic transmission but slows kinetics of mEPSCs

(A) Increased excitatory miniature synaptic activity in slices from 4E-BP2−/− mice. Left: Traces of mEPSCs from 4EBP2−/− and wild type mice. Right: Cumulative probability plots and summary bar graph for all cells showing increases in mEPSC amplitude, charge and frequency. (N=6 neurons/genotype and 200 events/neuron; data are means ± SEM. $p < 0.05$. Kolmogorov-Smirnov test). (B) Expression of deamidated or wild type 4E-BP2 in 4E-BP2−/− neurons. Left: mEPSC traces from 4E-BP2−/− organotypic slices transfected with empty vector (vec), wildtype 4E-BP2, or deamidated 4E-BP2 (N99D/N102D). Transfected cells were identified by IRES-mediated eGFP expression from the same plasmid encoding 4E-BP2 variants. Right top: Cumulative probability plots of mEPSC amplitude, charge, and frequency. Right bottom: Summary of effects on mEPSC amplitude, charge and frequency. (N=6 neurons/condition and 150 events/neuron; * $p < 0.05$, ** $p < 0.01$. One-way ANOVA). (C) Partial repression of mEPSC charge by deamidated 4E-BP2 is associated with slower kinetics. Top: Individual (10 traces, grey) and averaged (150 events, black) mEPSCs from neurons transfected as in (B). Superimposed scaled responses of average mEPSCs, are at the right. Bottom left: Cumulative probability plots for 10-90% rise and 90-10% decay times for all groups ($p < 0.05$, Kolmogorov-Smirnov test). Bottom right: Summary bar graphs of rise and decay times. (N=6, $p < 0.01$. One-way ANOVA). See also Figure S6.